Preparation and Characterization of Pu and Hf Bearing Lanthanide Boroilicate and Aluminoborosilicate Glasses – 15667

Sergey Stefanovsky **, Olga Stefanovsky *, Boris Nikonov ***, James Marra ****
* FSUE RADON
** Frumkin Institute of Physical Chemistry and Electrochemistry
*** Institute of Geology of Ore Deposits
**** Savannah River National Laboratory

ABSTRACT

Eight borosilicate glasses with LaBS and ABS compositions containing plutonium and/or hafnium as a plutonium surrogate were prepared in Pt ampoules (Pu-bearing) and alumina or Pt crucibles (Hf-bearing) and characterized by X-ray diffraction, optical and scanning electron microscopy, infrared and Raman spectroscopy. Hf-bearing LaBS glasses were found to be amorphous whereas Pu-bearing glasses contained trace of plutonium dioxide and britholite. Hf and Fe bearing ABS glasses contained minor spinel structure phase. As followed from optical and SEM studies Hf-bearing LaBS glasses were more homogeneous than Pu-bearing and ABS glasses. The structure of the anionic motif of the glasses investigated by IR and Raman spectroscopy is typical of the glasses with relatively low silica content.

INTRODUCTION

Actinide oxides normally have low solubility in borosilicate glasses. Solubility limit for PuO_2 in a sodium trisilicate glass is ~8 wt.%. Maximum PuO_2 and AmO_2 concentrations in complex borosilicate glasses were found to be about 2 wt.%. Solubility limits decrease with increasing atomic number and decreasing ionic radius at the same valence [1]. Due to low PuO_2 and AmO_2 solubility in conventional borosilicate glasses to increase Pu/Am-bearing wastes loading special compositions of the glasses were designed [2-11] or melting under reducing conditions to convert Pu(IV) to Pu(III) was suggested [12]. The alkali-tin-silicate, ATS [2] and lanthanide-borosilicate, LaBS [3,4] glasses are capable to dissolve up to ~10 wt.% PuO_2 without its segregation in a separate phase. Higher PuO_2 solubility as compared to conventional borosilicate waste glasses may be due to modification of the glass network caused by the incorporation of larger-sized lanthanide cations. The melting temperature of the ATS glass is the same as of conventional borosilicate waste glasses (~1100 °C); whereas, the melting point for the LaBS glass is much higher (~1400 °C). The LaBS-type glasses were developed for immobilization of the (Am,Cm)-containing Savannah River Plant waste. They are produced by melting an ABS frit and lanthanide and actinide oxides [5]. LaBS glasses are more durable in water solutions than conventional borosilicate glasses [6].

There is limited information about the structure of the LaBS glasses. It has been found that the as-prepared glasses may contain trace of undissolved PuO_2 [13] and britholite [14-16]. Thermal treatment at 1250 °C and even storage at room temperature for 1 year and longer time resulted in crystallization of PuO_2-HfO_2 solid solution [13] and extra PuO_2 and britholite [14- 16]. Pu in LaBS glasses is predominantly tetravalent [17] and being partitioned between vitreous and crystalline phase (mainly PuO_2) has different co-ordination environment which can be also varied in time [16,17].

Hf(IV) is used as both a neutron absorber and a surrogate for Pu(IV). In sodium boro-alumino-silicate glasses with molar $Na_2O>Al_2O_3$, i.e., peralkaline glasses, the solubility limit of hafnia is linearly and positively correlated with excess sodium, represented by $Na_2O/(Na_2O+Al_2O_3)$ or Na_2O/Al_2O_3 and maximum HfO_2 content was found to be ~16 mol.% [18].

In the present work we continue our study of the structure of the LaBS glasses [13-17] using both actual Pu and Hf as its surrogate.

EXPERIMENTAL

Frit compositions for Pu immobilization were designed at Savannah River National Laboratory [11]. Target chemical compositions of the glasses studied are given in Table I. The glasses #1 and #3 contained actual Pu whereas the others – Hf as a Pu surrogate.

Table I. Target Chemical Compositions of the LaBS Glasses.

Oxides	Frit X with PuO_2 (1)		Frit X with HfO_2 (2)		Frit X with PuO_2 (3)		Frit X with HfO_2 (4)		Frit A with HfO_2 (5)		Frit A with HfO_2 (6)		Frit ABS with HfO_2 (7)		Frit ABS with HfO_2 (8)	
	mol.%	wt.%	mol.%	wt.%	mol.%	wt.%	mol.%	wt.%	mol.%	wt.%	mol.%	wt.%	mol.%	wt.%	mol.%	wt.%
Li_2O	-	-	-	-	-	-	-	-	-	-	-	-	10.8	4.9	10.9	5.0
B_2O_3	21.8	11.8	21.8	12.0	22.4	12.4	22.4	12.5	16.2	10.8	16.5	11.2	5.6	5.9	5.6	6.0
Na_2O	-	-	-	-	-	-	-	-	-	-	-	-	14.6	13.8	14.7	14.0
Al_2O_3	11.4	9.0	11.4	9.2	11.8	9.5	11.8	9.6	20.3	19.8	20.7	20.7	5.7	8.8	5.7	8.9
SiO_2	39.1	18.1	39.1	18.6	39.9	19.0	39.9	19.2	46.8	27.0	47.7	28.0	53.7	49.1	53.9	49.7
CaO	-	-	-	-	-	-	-	-	-	-	-	-	2.4	2.0	2.3	2.0
MnO	-	-	-	-	-	-	-	-	-	-	-	-	1.9	2.0	1.8	2.0
Fe_2O_3	-	-	-	-	-	-	-	-	-	-	-	-	4.9	11.9	4.9	12.0
SrO	2.9	2.3	2.9	2.4	2.9	2.4	2.9	2.4	2.4	2.4	2.4	2.4	-	-	-	-
ZrO_2	-	-	-	-	-	-	-	-	1.0	1.2	1	1.2	-	-	-	-
La_2O_3	6.8	17.2	6.8	17.5	7.0	18.1	7.0	18.3	3.7	11.4	3.8	11.9	-	-	-	-
Nd_2O_3	5.2	13.6	5.2	13.8	5.3	14.3	5.3	14.4	3.7	11.9	3.7	12.4	-	-	-	-
Gd_2O_3	4.4	12.2	4.4	12.6	4.5	12.8	4.5	13.0	2.3	8.0	2.3	8.3	-	-	-	-
HfO_2	3.9	6.3	8.4	14.0	4.0	6.7	6.3	10.7	3.7	7.5	1.9	3.8	0.5	1.6	0.1	0.4
PuO_2	4.5	9.5	-	-	2.3	5.0	-	-	-	-	-	-	-	-	-	-
Sums	100.0	100.	100.0	100.0	100.0	100.0	100.0	100.0	100.0	100.0	100.0	100.0	100.0	100.0	100.0	100.0

Glasses were prepared from reagent-grade Al_2O_3, H_3BO_3, SiO_2, La_2O_3, Nd_2O_3, Gd_2O_3, $CaCO_3$, $SrCO_3$, ZrO_2, HfO_2, MnO, Fe_2O_3, $LiOH{\cdot}H_2O$, $NaNO_3$. Chemicals were intermixed in an agate mortar and mechanically treated/activated in an AGO-2U planetary mill. Pu-bearing samples were produced from mechanically activated precursor impregnated with a plutonium nitrate solution followed by drying of the mixture under infrared (IR) lamp and calcining in a Pt crucible at a temperature of 600 °C for 3 hrs. The Hf-bearing mixtures in amount of ~10 g each were charged in either alumina or platinum crucibles which were heated in a resistive furnace to a temperature of 1500 °C at a rate of 10 °C/min followed by keeping for 30 min and quenching of the melts onto a stainless steel plate.

The Pu-bearing calcines in amount of ~500 mg were filled in Pt ampoules, which were sealed and heated in a resistive furnace using same regime as for the Hf-bearing mixtures. Then ampoules were removed from the furnace and cooled down to room temperature in air.

The glasses produced were examined with X-ray diffraction (XRD) using a Rigaku D/MAX-2200 diffractometer (Cu Kα radiation), optical microscopy using an OLYMPUS BX51 polarizing microscope (polished sections were prepared by smoothing on rotating mechanical disc using abrasives with grain size from 0.105 to 0.003 mm followed by polishing with a felt), scanning electron microscopy (SEM) using a Tescan Vega II XMU unit with an INCAx-sight energy dispersive X-ray (EDX) spectrometer, IR

spectroscopy using a modernized IKS-29 spectrophotometer (compaction of powdered glass in pellets with KBr), and Raman spectroscopy using a Jobin Yvon U1000 spectrophotometer (excitation wavelength is 514,4 Å).

RESULTS

XRD

As follows from XRD patterns (Figure 1) the as-prepared glasses ##2 to 6 produced in Pt crucibles are fully amorphous. The glass #1 with ~9.5 wt.% PuO_2 contains minor crystalline PuO_2 and trace of britholite but their amounts are lower than those found in the samples studied in our previous works [13-15] due to higher cooling rate. The glasses ## 2, 4, 5 and 6 produced in alumina crucibles were also amorphous. The Fe-bearing samples ## 7 and 8 produced in both Pt and alumina crucibles contain minor spinel structure phase with a chemical composition close to magnetite as it is seen from location of the strongest reflections at d_{311} = 2.512-2.513 Å, d_{220} ≈2.961 and d_{400} ≈ 2.100.

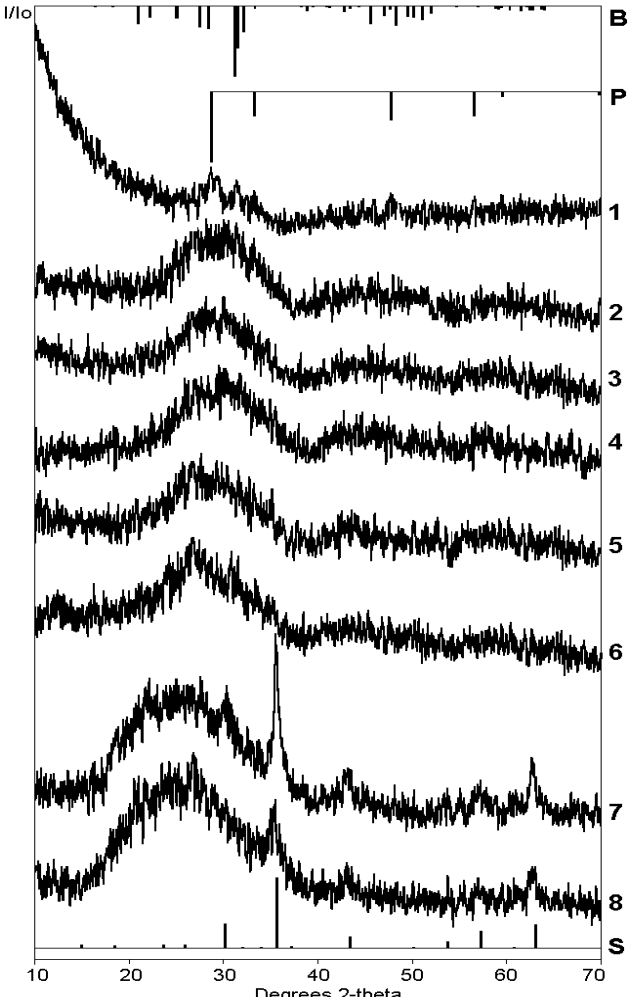

Figure 1. XRD patterns of the glasses.
1-8 – Glass ID in Table I, B – britholite, P – PuO_2, S – spinel.

Optical and electron microscopy

Optical microscopic images demonstrate high homogeneity of the samples ## 2, 4, 5 and 6 produced in both Pt and alumina crucibles (Figure 2). The glasses are visually transparent and have light-lilac color with a typical conchoidal fracture. They are clear and uniform in transparent microsections (Figure 2, *1,3,6,7*) and isotropic in crossed Nichols (Figure 2, *2,4,5*). In crossed Nichols low double refracting elongated or cross-like areas on the background of isotropic glass rarely occur. They are characterized by non-uniform wavy extinction. These areas may be suggested to be crystallites formed at the initial stage of glass devitrification. Major optical difference between crystallites and crystals are blurry contours and non-uniform wavy extinction at rotation of microscope's table at crossed Nichols. The microsections of all the glasses are threaded with fractures pointing to high mechanical stresses in glasses.

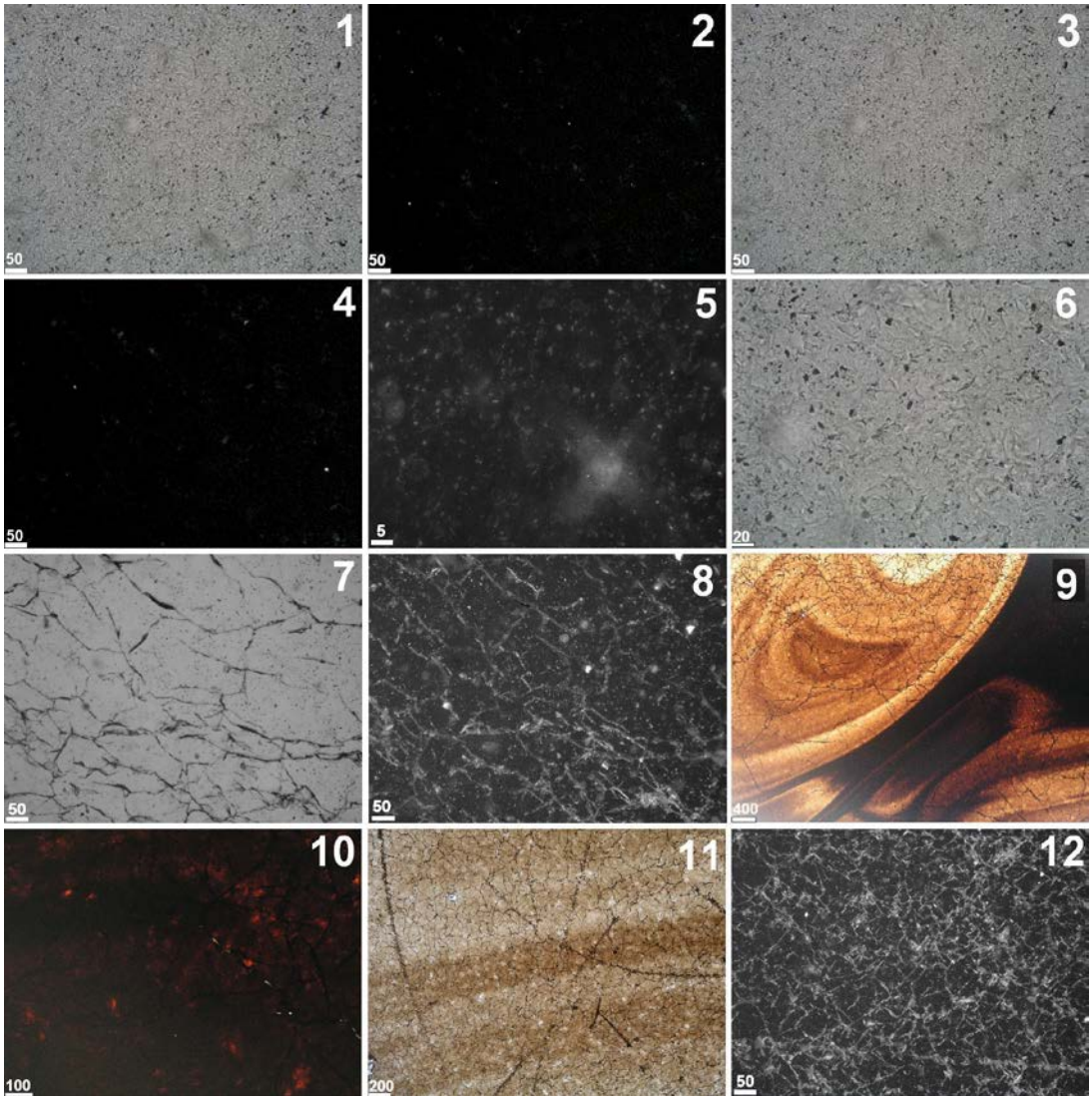

Figure 2. Optical Microscopic Images of the Glasses ##2 (1,2), 4 (3,4,5), 6 (6), 7 (7,8,9,10), and 8 (11,12) in Parallel (1,3,6,7,9,11) and Crossed Nichols (2,4,5,8,10,12). Glass ID is given in Table I. Scale bars are given in microns.

The quenched glass #7 demonstrates uniform texture in its bulk (Figure 2, *7,8*) whereas near-surface zone of same glass has layered structure and irisation pointing to formation of very fine crystals (crystallites) with a size of ≤100 nm (Figure 2, *9*). The layers are different in color which varies from light-brown to dark-brown, nearly black. Some layers are occasionally split and crop out.

"Web" of microfractures testifies about high residual mechanical stresses in the glass. In crossed Nichols there are fine inclusions which are lighter than darker, nearly black, background and can be attributed to microcrystals of spinel (Figure 2, *10*).

The glass #8 is rather uniform (Figure 2, *11,12*). Layered texture is not clearly appeared but brown bands on the background of light-brown glass are quite discernible. Similarly to the previous sample a "web" of microfractures points to high stress in the glass.

SEM images demonstrate good agreement with optical microscopy data. While the glass #1 contains minor pyrochlore and/or britholite (Fig. 3, *1*) the glasses ## 2, 4, 5 and 6 were found to be fully homogeneous (Figure 3, *2-4*). Fine defects arose at polishing. As seen from Table II, the glasses with relatively low target Al_2O_3 content produced in alumina crucibles are enriched with Al_2O_3 due to its dissolution in borosilicate melts. For the high- Al_2O_3 glasses the difference between the target and actual Al_2O_3 contents is negligible. The glasses produced in Pt crucibles have chemical composition close to the target one.

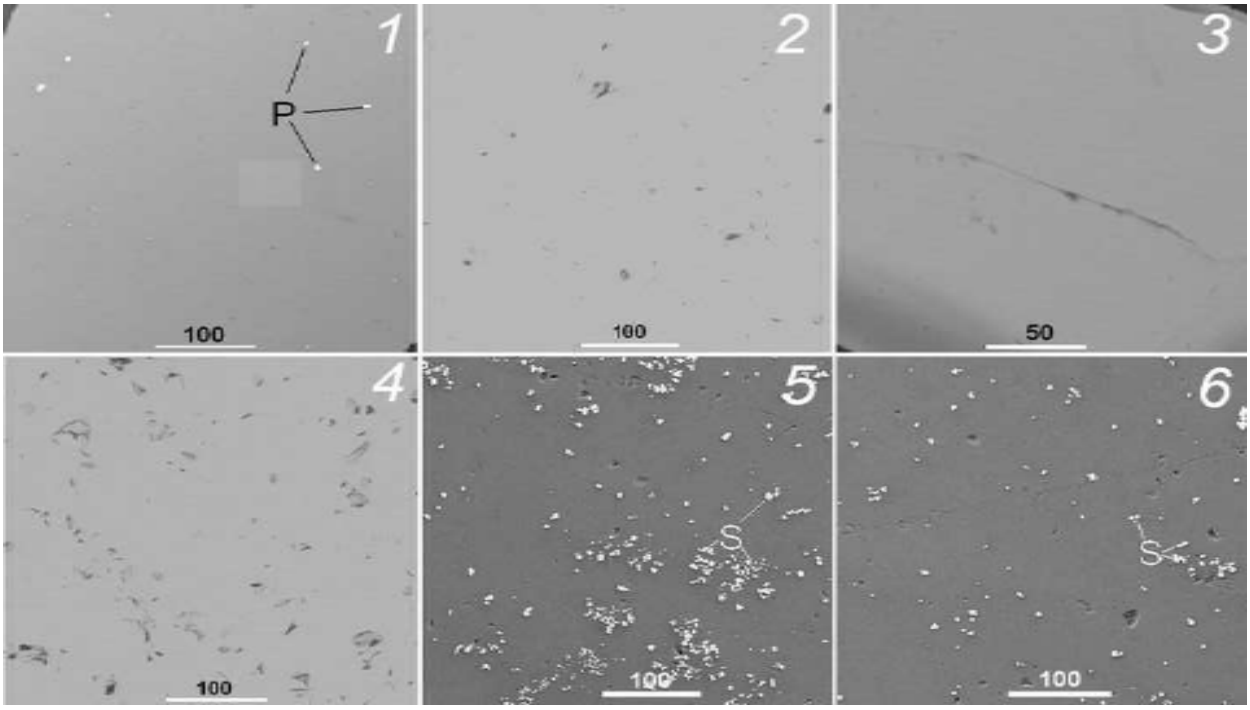

Figure 3. SEM Images in Backscattered Electrons of the Glasses ## 1 (1), 2 (2), 5(3), 6 (4), 7 (5), and 8 (6) Produced in Platinum Crucibles.
Glass ID is given in Table I. Scale bars are given in microns. P – pyrochlore/britholite, S – spinel.

Glasses #7 (Figure 3, *5*) and #8 (Figure 3, *6*) are less uniform. In both the glasses the vitreous matrix is rather homogeneous but fine individual and chain-type aggregated white inclusions also occurred. They may be assigned to crystals of the spinel phase occurred in the samples and that was confirmed by XRD

data. Precise determination of chemical composition of the spinel crystals is impossible due to small crystal size and only bulk chemical composition may be determined (Table II). Similarly to the glasses ##2, 4, 5, 6 extra Al_2O_3 is present in the glasses produced in alumina crucibles due to Al_2O_3 dissolution in borosilicate melts. Oxide concentrations in the glasses produced in platinum crucibles are close to the target values and the glasses are more homogeneous. Thus, glasses with relatively low Al_2O_3 content cannot be produced in alumina crucibles and require platinum crucibles for their preparation.

Table II. Chemical Compositions (wt.%) of Glasses #2, #6, #7 and #8 Produced in Alumina (Al) and Platinum (Pt) Crucibles Determined by EDX.

	2			6			7			8		
Oxides	Target	Al	Pt	Target	Al	Pt	Target	Al	Pt	Target	Al	Pt
Li_2O*	-	-	-	-	-	-	4.9	4.6	4.9	5.0	4,7	5.0
B_2O_3*	12.0	4.8	11.7	11.2	7.3	10.9	5.9	5.6	5.9	6.0	5,6	6.0
Na_2O	-	-	-	-	-	-	13.8	10.0	13.8	14.0	10,5	13.9
Al_2O_3	9.2	23.7	9.3	20.7	22.5	20.9	8.8	27.8	8.9	8.9	26,9	9.0
SiO_2	18.6	18.7	18.7	28.0	33.5	28.1	49.1	39.1	49.2	49.7	40,7	49.7
CaO	-	-	-	-	-	-	2.0	1.6	2.0	2.0	1,7	2.0
MnO	-	-	-	-	-	-	2.0	1.6	2.1	2.0	1,4	2.0
Fe_2O_3 /FeO	-	-	-	-	-	-	11.9	8.3	12.0	12.0	8,0	12.1
SrO	2.4	1.7	2.4	2.4	2.9	2.4	-	-	-	-		-
ZrO_2	-	-	-	1.2	1.4	1.3	-	-	-	-		-
La_2O_3	17.5	15.5	17.6	11.9	11.1	12.0	-	-	-	-		-
Nd_2O_3	13.8	11.6	13.8	12.4	10.6	12.4	-	-	-	-		-
Gd_2O_3	12.6	11.4	12.6	8.3	7.2	8.3	-	-	-	-		-
HfO_2	14.0	12.6	13.9	3.8	3.5	3.9	1.6	1.3	1.6	0.4	0,6	0.5
Sums	100.0	100.0	100.0	100.0	100.0	100.0	100.0	100.0	100.4	100.0	100,0	100.2

* Li and B are not determined by EDX; for glasses #2 and #6 B_2O_3 concentrations were calculated by difference 100% - Sum of other oxides; for glasses #7 and #8 the target values are given.

IR and Raman Spectroscopy

IR spectra of the glasses produced in Pt crucibles are shown on Figure 4. In the spectra of both glasses weak absorption bands due to absorbed or crystallized water in the high wavenumber range (ν_{as} ~3400-3600 cm^{-1} and ν_S ~1600-1650 cm^{-1}) are present. Weak absorption around 2800-2900 cm^{-1} is due to vibrations of hydrogen bonds (Figure 4, left).

Within the range lower 1600 cm^{-1} strong absorption bands are due to vibrations of the chemical bonds in the anionic motif of the glass network (Figure 4, right). IR spectra of all the glasses studied within this range consist of strong broad bands at 850-1200 cm^{-1} and 400-600 cm^{-1} and weaker bands at 1200-1500 cm^{-1} and 600-800 cm^{-1}. The bands are split into several components due to superposition of the bands caused by major vibrations in various silicon-oxygen, boron-oxygen, and aluminum-oxygen groups in vitreous phase and minor vibrations of the bonds in crystals. This splitting is mostly typical of the spectra of glasses ## 1-3 (Figure 4).

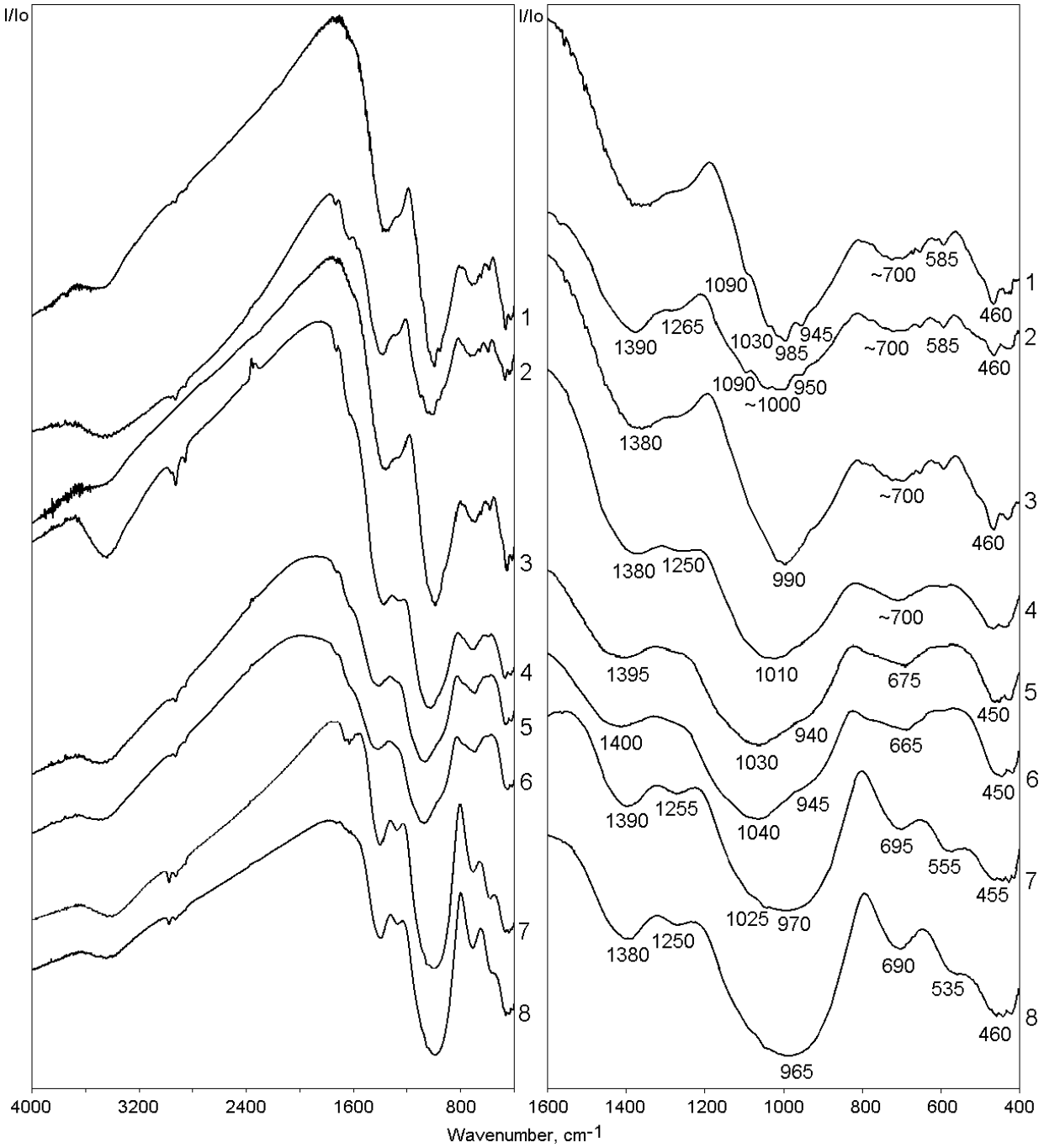

Figure 4. IR Spectra of the LaBS Glasses Produced in Pt Crucibles. 1-8 – Glass ID in Table I.

Maximum of the band within the range of 800-1200 cm^{-1} in IR spectra of the materials with Frits X, A and ABS is positioned at about 1000 cm^{-1}, 1030-1040 cm^{-1}, and ~970 cm^{-1}, respectively. At that, this band in spectra of the glasses with Frit X is multicomponent (mainly in spectra of the glasses ##1-3), with Frit A consists of two major components at 1030-1040 cm^{-1} and 940-945 cm^{-1}, and with Frit ABS is nearly structureless.

Within the range of 1200-1500 cm^{-1} in IR spectra of glasses with Frit X the band with a maximum near 1400 cm^{-1} is stronger than that of 1250-1270 cm^{-1} whereas in spectra of glasses with Frit A the latter looks like a shoulder and in spectra of the materials with Frit ABS its intensity is comparable with that of higher wavenumber band.

Raman spectra of all the glasses produced in Pt crucibles except glass #1 (Figure 5) contain strong bands within the range of 850-1150 cm^{-1} with maxima at 950-970 cm^{-1} and lower 700 cm^{-1} due to stretching and bending modes in SiO_4 tetrahedra and weaker bands at 1300-1500 cm^{-1} due to stretching modes in BO_3 and complex borate groups [19-22]. Raman spectra of Pu- bearing glass #1 and, in much less extent, glass #3 contain the bands including the strongest band with a maximum at 844-850 cm^{-1} typical of orthosilicate units in the apatite structure [23-25]. The band at 850-1150 cm^{-1} in the spectra of the glasses #7 and #8 prepared using Frit ABS is markedly asymmetric. Moreover a weak absorption within the range of 700-800 cm^{-1} is present (Figure 5, *7, 8*).

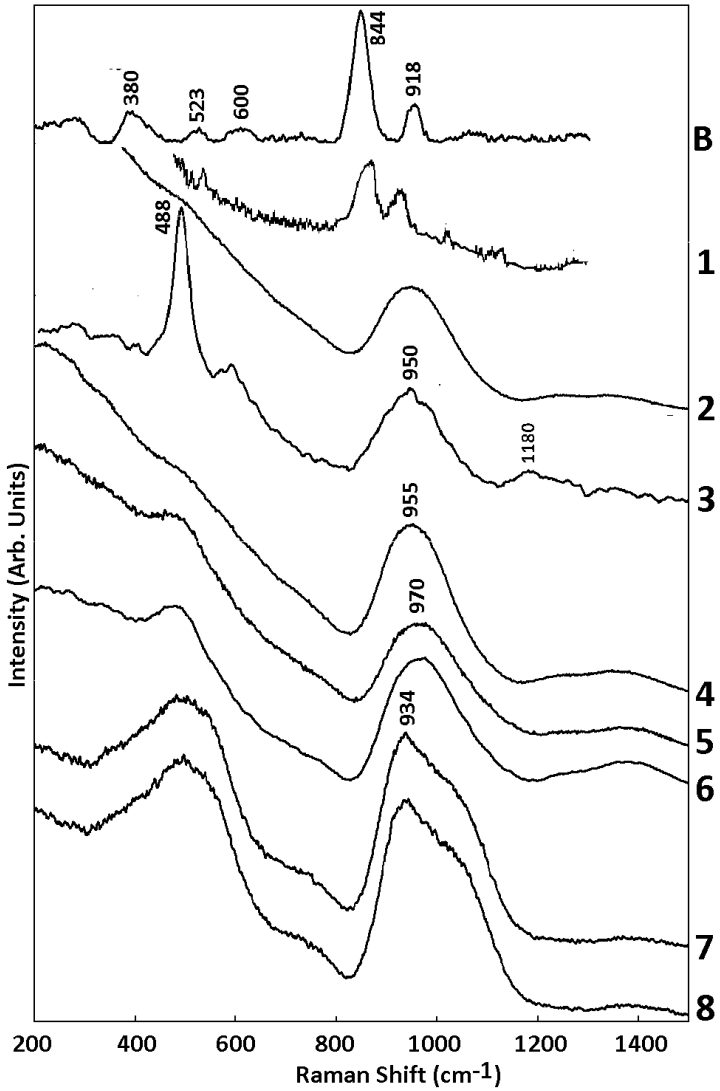

Figure 5. Raman Spectra of LaBS Glasses Produced in Pt Crucibles.

1-8 – Glass ID in Table I, B – britholite

DISCUSSION

All the materials studied are mainly amorphous and homogeneous and may be considered as glasses. Pu-bearing glasses produced using Frit X (#1 and #3) contain minor britholite and PuO_2 or PuO_2-based solid solution. HfO_2 is higher soluble in borosilicate melts than PuO_2 [1-11] and no crystalline phases in the HfO_2-bearing glasses have been found.

In both IR (Figure 4) and Raman spectra (Figure 5) of the glasses the wavenumber ranges of 1300-1500 cm^{-1} (with a maximum at ~1370 cm^{-1}) and ~1230-1270 cm^{-1} are typical of vibrations in the boron-oxygen groups with trigonally coordinated boron (boron-oxygen triangles BO_3) [19-22,26-30]. These bands were attributed to components of twice degenerated asymmetric valence ν_3 O−B−O vibrations (stretching modes). The band with components 720 and 655-657 cm^{-1} are due to twice degenerated asymmetric deformation $\delta(\nu_4)$ O−B−O vibration (bending modes) [19]. Stretching ν_1 O−B−O modes at ~805-810 cm^{-1} are inactive in IR spectra but observable in Raman spectra [20] and may associate with the edge of the band at 800-890 cm^{-1} in the Raman spectrum of the Pu-bearing LaBS glasses. The shoulder at ~500 cm^{-1} and the band with a maximum at ~467-470 cm^{-1} are components of δ_S (ν_2) O−B−O bending modes. Their appearance exhibits distortion of BO_3 units linked in network.

Strong absorption in both IR and Raman spectra within the range of 850-1150 cm^{-1} is caused by asymmetric ν_3 vibrations in silicon-oxygen units linked to zero (850-900 cm^{-1}), one (~900-950 cm^{-1}), two (~950-1000 cm^{-1}), three (~1000-1050 cm^{-1}) and four (>1050 cm^{-1}) neighboring SiO_4 tetrahedra (Q^0, Q^1, Q^2, Q^3, Q^4, respectively) [21,22] and, in less extent, BO_4 tetrahedra (1030 cm^{-1}). The bands in IR spectra at ~595, ~460 and 432 cm^{-1} are due to bending modes in the SiO_4 units. The bands due to vibrations of Al-O bonds in AlO_4 units are positioned within the range of 700-850 cm^{-1} [31] and overlapped with strong bands due to vibrations of B-O and Si-O bonds.

Both IR and Raman spectra of the glasses based on Frit A demonstrate dominance of meta- (Q^2) and pyrosilicate (Q^1) units in their structure and major ternary-coordinated boron whose units form local structures having a tendency to chemical ordering. Fraction of ternary- coordinated boron increases at low Al_2O_3 content, when both Al and B become tetrahedrally coordinated for oxygen [32]. The band with a maximum at ~650-750 cm^{-1} is a characteristic of [AlO_4] units [20,30]. Moreover Raman spectrum of the glass #1 demonstrates appreciable contribution of the spectrum due to britholite whose occurrence in the sample was revealed by XRD.

IR spectra of the glasses ##7 and 8 with high Fe_2O_3 content are similar to those of borosilicate glasses for immobilization of Savannah River Site SB2 and SB4 high level waste surrogates [33,34]. The anionic motif of these glasses is built from meta- and shorter pyrosilicate chains with minor fraction of [SiO_4] units with higher degree of connectedness (the band at ~1025 cm^{-1}). The splitting of the band in this range may also be due to the effect of highly charged cations (Fe^{3+}, Al^{3+}). Occurrence in the IR spectra of these glasses the band with a maximum at 535-555 cm^{-1} due to vibrations of Fe^{3+}-O bonds, which is absent in the spectra of Fe-free glasses ##1-6, and splitting of the band at 400-500 cm^{-1} testifies in favor of contribution from vibrations in the structure of fine spinel crystals. Stretching vibrations of Ln-O bonds positioned at 450-480 cm^{-1} [35,36] probably make some contribution to the band at 400-500 cm^{-1} and these are overlapped with stronger bending modes in SiO_4 tetrahedra.

In silicate glasses the Ln^{3+} ions act as network-modifiers increasing the fraction of SiO_4 tetrahedra with the lower number of bridging oxygens thus resulting in depolymerization of glass network [37,38]. In borosilicate glasses Gd^{3+} ions increase the fraction of the BO_3 units and first partition to the borate-rich environment following by excess Gd cations enter silicate-rich one [39]. In the Frit X and Frit A based glasses total Ln_2O_3 concentration reaches ~45 wt.% (~17 mol.%) and ~32 wt.% (~10 mol.%),

respectively, therefore Gd^{3+} (and probably La^{3+} and Nd^{3+}) ions are linked with both boron-oxygen and silicon-oxygen fragments of the glass network. This is in good agreement with data of our previous work for Pu [16] and a model suggested in [22].

On the whole, the glasses based on Frit X are the most structured and have a tendency to chemical differentiation with formation of chemically and structurally ordered microareas as it is seen from the splitting of absorption bands in IR spectra. Storage of these glasses in air for ~3 yrs resulted in surface devitrification with segregation of the britholite and PuO_2-HfO_2 solid solution phases especially in glass #3 [17]. Glasses produced with Frits A and ABS have higher polymerized network.

CONCLUSION

Glasses for Pu immobilization were prepared using three Frit compositions: REE_2O_3- bearing aluminoborosilicate Frit X, high-Al_2O_3 REE_2O_3-bearing aluminoborosilicate Frit A, and lithium-sodium borosilicate Frit ABS. The as-prepared Frit X based glass with 9.5 wt.% PuO_2 (#1) contained trace of PuO_2 and britholite, the Frit X and Frit A based glasses ## 2-6 were fully amorphous, although glass #3 (5.0 wt.% PuO_2) may contain trace of PuO_2 and britholite as well. Glasses ##7 and 8 (Fe-bearing) produced using Li-Na-B-Si Frit ABS contained minor spinel structure phase or crystallites formed at the early stage of crystallization. HfO_2 seems to be some more soluble in borosilicate glasses than PuO_2 and Hf-bearing glasses were found to be more homogeneous than the Pu-bearing at the same molar oxide concentrations of HfO_2 and PuO_2. Incorporation of Fe_2O_3 in the LaBS glasses results in textural non-uniformity of the glasses and formation of microcrystals of magnetite-type spinel. As follows from IR and Raman spectra the glasses based on Frit X are the most structured and have a tendency to chemical differentiation with formation of chemically and structurally ordered microareas as it is seen from the splitting of absorption bands in IR spectra. Raman spectrum of the glass with the highest PuO_2 content demonstrates appreciable contribution of the spectrum due to britholite. The glasses based on Frit A are much more homogeneous; glasses based on Frit ABS have compositionally uniform matrix with minor fine spinel crystals distributed within its bulk and their anionic motif is closer on structure to borosilicate glasses containing high-Fe SRS SB2 and SB4 surrogates

REFERENCES

1. B.W. VEAL, J.N. MUNDY, D.J. LAM, *Handbook of the Physics and Chemistry of Actinides,* pp. 271- 309, A.J. Freeman and G.H. Lander, Eds., Elsevier Science Publishers B.V., The Netherlands (1987).
2. M.J. PLODINEC, *Development of Glass Compositions for Immobilization of SRP Waste*, DP 1517, Savannah River Site, Aiken (1979)**.**
3. C.T. WALKER, U. RIEGE, *Ceramics in Nuclear Waste Management*, pp. 198-202, T.D. CHIKALLA and J.E. MENDEL, Eds., CONF-790420 (1979).
4. D.B. CHAMBERLAIN, J.M. HANCHAR, J.W. EMERY, J.C. HOH, S.F. WOLF, R.J. FINCH, J.K. BATES, A.J.G. ELLISON, and D.B. DINGWELL, *Mater. Res. Soc. Symp. Proc.* **465**, 1229 (1997) .
5. N.E. BIBLER, W.G. RAMSEY, T.F. MEAKER, and J.M. PAREIZS, *Mater. Res. Soc. Symp. Proc.* **412**, 65 (1996).
6. M.G. MESKO, T.F. MEAKER, W.G. RAMSEY, J.C. MARRA, and D.K. PEELER, *Mater. Res. Soc. Symp. Proc*. **465**, 105 (1997).
7. B.J. RILEY, J.D. VIENNA, M.J. SCHWEIGER, D.K. PEELER, and I.A. REAMER, *Mater. Res. Soc. Symp. Proc*. **608** (2000) 677-682.

8. D.M. STRACHAN, A.J. BAKEL, E.C. BUCK, D.B. CHAMBERLAIN, J.A. FORTNER, C.J. MERTZ, S.F. WOLF, W.F. BOURCIER, B.B. EBBINGHAUS, H.F. SHAW, R.A. VAN KONYNENBURG, B.P MCGRAIL., J.D. VIENNA, J.C. MARRA, and D.K. PEELER, Proc. Waste Management '98 Conf., Laser Options Inc., Tucson, AZ, 1998. ID 65-08, CD-ROM.
9. I. MULLER and W. WEBER, *Mater. Res. Soc. Bull*. [9] 698 (2001).
10. M.T. HARRISON, C.R. SCALES, P.A. BINGHAM, and R.J. HAND, *Mater. Res. Soc. Symp. Proc*. **985**, 151 (2007).
11. C.L. CRAWFORD, J.C. MARRA, and N.E. BIBLER, Glass Fabrication and Product Consistency Testing of Lanthanide Borosilicate Glass for Plutonium Disposition, *J. Alloy Compd*., **444- 445**, 569 (2007).
12. J.-N. CACHIA, X. DESCHANELS, C. DEN AUWER, O. PINET, J. PHALIPPOU, C. HENNIG, and A. SCHEINOST, J. Nucl. Mater. 352, 182 (2006).
13. K.I. MASLAKOV, S.V. STEFANOVSKY, A.YU. TETERIN, YU.A. TETERIN, and J.C. MARRA, *Glass Phys. Chem*. **35**, 22 (2008).
14. A.A. SHIRYAEV, Y.V. ZUBAVICHUS, S.V. STEFANOVSKY, A.G. PTASHKIN, and J.C. MARRA, *Mater. Res. Soc. Symp. Proc*. **1193**, 259 (2010).
15. S.V. STEFANOVSKY, A.G. PTASHKIN, A.A. SHIRYAEV, J.V. ZUBAVITCHUS, A.A VELIGJANIN, J. MARRA, and M.V. CHUKALINA, *Ceram. Trans*. **217**, 17 (2010).
16. S.V. STEFANOVSKY, A.A. SHIRYAEV, Y.V. ZUBAVICHUS and J.C. MARRA, *Mater. Res. Soc. Symp. Proc*. **1264**, 21 (2010).
17. S.V. STEFANOVSKY, A.A. SHIRYAEV, I.E. VLASOVA, V.O. YAPASKURT, and J.C. MARRA, *Mater. Res. Soc. Symp. Proc*. **1444**, 223 (2012).
18. L.L. DAVIS, J.G. DARAB, M. QIAN, D. ZHAO, C.S. PALENIK, H. LI, D.M. STRACHAN, and L. LI, *J. Non-Cryst. Solids*. **328**, 102 (2003).
19. V.A. KOLESOVA, *Glass Phys. Chem*. (Russ.) **12**, 4 [1] (1986) .
20. K. NAKAMOTO, *Infrared and Raman Spectra of Inorganic and Coordination Compounds*, Sixth ed., A John Wiley and Sons, Inc., Hoboken, NJ (2009).
21. V.N. ANFILOGOV, V.N. BYKOV, and A.A. OSIPOV, *Silicate Melts* (Russ.), Nauka, Moscow, (2005).
22. D. CAURANT, P. LOISEAU, O. MAJERUS, V. AUBIN-CHEVALDONNET, I. BARDEZ, and A. QUINTAS, *Glasses, Glass-Ceramics and Ceramics for Immobilization of Highly Radioactive Nuclear Wastes*, Nova Science Publishers, Inc., New York, (2009).
23. RRUFF Project database, http://rruff.info.
24. E. RODRIGUEZ-REYNA, A.F. FUENTES, M. MACZKA, J. HANUZA, K. BOULAHYA, and U. AMADOR, *J. Solid State Chem*. **179**, 522 (2006) .
25. A. KIDARI, M. MAGNIN, R. CARABALLO, M. TRIBET, F. DOREAU, S. PEUGET, J.-L. DISSOSSOY, I. GIBOIRE, CH. JÉDOU, *ATALANTE 2012 Scientific Highlights*, 83 (2012).
26. D.A. MCKEOWN, I.S. MULLER, A.C. BUECHELE, I.L. PEGG, and C.A. KENDZIORA, *J. Non-Cryst. Solids* **262**, 126 (2000).
27. W.L. KONIJNENDIJK, *Philips Res. Repts Suppl*. [1] 1 (1975).
28. E.I. KAMITSOS and M.A. KARAKASSIDES, *Phys. Chem. Glasses*, **30** [1] 19 (1989).
29. K. EL-EGILI, *Physica B*, **325**, 340 (2003).
30. C. GAUTAM, A.K. YADAV, A.K. SINGH, International Scholarly Research Network, ISRN Ceramics (2012) ID 428497, doi: 10.5402/2012/428497.
31. I.I. PLUSNINA, *Infrared Spectra of Minerals*, MGU Publ., Moscow (1977).
32. A.A. APPEN, *Chemistry of Glass* (Russ.), Khimiya, Leningrad, USSR (1974).
33. S.V. STEFANOVSKY, B.S. NIKONOV, J.C. MARRA, *Glass Phys. Chem*. **34** [3] 333 (2008).
34. A.A. AKATOV, B.S. NIKONOV, B.I. OMEL'YANENKO, S.V. STEFANOVSKY, and J.C.

MARRA, *Glass Phys. Chem*. **35** [3] 243 (2009) .
35. S. SINGH, S.K. SINGH, S.C. SINGH, and R. DHAKAREY, *Asian J. Chem*. **16** [1] 117 (2004).
36. J. COELHO, N.S. HUSSAIN, P.C. GOMES, M.P. GARCIA, M.A. LOPES, M.H. FERNANDES, and J.D. SANTOS, *Current Trends on Glass and Ceramic Materials*, pp. 87-115, Bentham Science Publishers (2012).
37. J.R. FERRARO, J.J. HAZDRA, and W. BOETTNER, *J. Chem. Phys*. **57**, 4540 (1972) .
38. A.J.G. ELLISON and P.C. HESS, *J. Geophys. Res*. 95 (1990) 15717-15726.
39. H. LI, Z. WANG, L. LI, D.M. STRACHAN, Y. SU, and A.G. JOLY, *Mater. Res. Soc. Symp. Proc.* **702**, U8.1.1 (2002). DOI:10.1557/PROC-702-U8.1.1.

ACKNOWLEDGEMENTS

The work was performed under financial support from Savannah River National Laboratory.